

HIGHLY ANISOTROPIC MnBi MAGNETS

Nguyen Van Vuong^{*}, Nguyen Xuan Truong

*Institute of Materials Science, Vietnam Academy of Science and Technology,
18 Hoang Quoc Viet, Cau Giay, Hanoi*

^{*}Email: *vuongnv@ims.vast.ac.vn*

Received: 30 August 2015; Accepted for publication: 28 October 2015

ABSTRACT

The rare-earth-free MnBi magnetic material is promising for high-temperature ($150 \div 200$ °C) application of permanent magnets because of its large magnetocrystalline energy and especially the positive thermal coefficient of coercivity ($dH_c/dT > 0$). Because of the moderate value of the spontaneous magnetization $M_s \sim 74$ emu/g, the anisotropy of MnBi bulk magnets should be investigated to enhance the remanence M_r . With large ratio M_r/M_s and appropriate microstructure, the squareness γ of MnBi magnets should have high value leading the remanent coercivity ${}_bH_c$ close to the intrinsic coercivity ${}_iH_c$, thus enhancing the energy product $(BH)_{\max}$. The paper presents an approach to loading and compacting of MnBi powders in the 18 kOe magnetic field oriented perpendicular to the pressing direction where MnBi grains can be freely rotated and oriented parallel to the field direction. Based on the energy minimization of the assembly of magnetized grains, the compacting pressure was chosen to optimize two parameters, the mass density ρ and the coercivity ${}_iH_c$ of magnets. The prepared MnBi bulk magnet had $\rho \sim 8.4$ g/cm³, $M_r/M_s \sim 0.92$, $\gamma \sim 0.89$ and $(BH)_{\max}$ reached ~ 8.4 MGOe.

Keywords: rare-earth-free MnBi magnets, anisotropy, anisotropic compaction.

1. INTRODUCTION

Large magnetocrystalline energy of $K \sim 0.9$ MJm⁻³ and positive thermal coefficient of coercivity ($dH_c/dT > 0$) make the rare-earth-free MnBi magnetic material appealing for producing low cost magnets used in the applications at an elevated high temperature in the range of $150 \div 200$ °C [1 - 5]. With the maximum value 8.2 kG of the spontaneous magnetization M_s and the perfect microstructure, the energy product $(BH)_{\max}$ of MnBi magnets can reach the room-temperature theoretical limit of 16.8 MGOe. In practice, $(BH)_{\max}$ of prepared MnBi magnets is far below this theoretical value. In 1952, the first MnBi bulk magnet was prepared by using the conventional metallurgical method, having $(BH)_{\max} = 4.5$ MGOe [6]. The spark plasma sintering technique used in [7] improves the magnet mass density but cannot increase the energy product because of the complexity of the phase diagram of Mn-Bi system, $(BH)_{\max}$ is only 2.4 MGOe. The hot compaction technique implemented in [8] enhanced $(BH)_{\max}$ up to 5.8 MGOe. The temperature gradient driven annealing together with the low-energy ball mill and the hot compaction improved $(BH)_{\max}$ to 6.1 MGOe [9]. By using the melt spun MnBi powders and the

hot compaction technique [10], the energy product was increased up to 6.7 MGOe. The low-temperature low-energy ball-mill and quick hot compaction techniques performed in [11] have further enhanced $(BH)_{\max}$ but only up to 7.8 MGOe.

In any bulk magnets, the energy product $(BH)_{\max}$ directly depends on the remanence M_r , the intrinsic coercivity iH_c , and the squareness γ . These three parameters depend strongly on the anisotropy of magnets, which is closely related to the unit cell structure of materials and strongly depends on the technology of magnet preparation. Therefore, a better way of increasing the anisotropy of magnets will directly improve the energy product.

This paper shows a way for preparing highly anisotropic MnBi bulk magnets which help the remanence M_r exceeding 90 % of M_s . This high anisotropy also contributes to increasing the squareness of the second quadrant demagnetization curve, consequently increasing $(BH)_{\max}$ of magnets. The compaction of anisotropic magnets was also performed by optimizing the interaction between magnetized ferromagnetic particles to prepare dense magnets with a good balance between M_r and iH_c in order to improve $(BH)_{\max}$. The prepared MnBi magnet had $\rho \sim 8.4 \text{ g/cm}^3$, $M_r/M_s \sim 0.92$, $\gamma \sim 0.89$ and $(BH)_{\max}$ reached the value of 8.4 MGOe.

2. EXPERIMENTS

To prepare high-performance Mn-Bi bulk magnets, because the ferromagnetic phase is $\text{Mn}_{50}\text{Bi}_{50}$ (referred to as the LTP – Low Temperature Phase of MnBi as this phase is formed only below 340 °C), the starting Mn and Bi materials were weighted by the atomic ratio 1:1 despite the lack of the eutectic point at this ratio on the phase diagram of Mn-Bi system [12]. From this phase diagram the phase segregations during the solidification are clearly observed. Therefore, in order to obtain samples with high LTP content δ , the arc-melted alloys must be annealed. The annealing temperature 300 °C was chosen, which is below the upper limit 340 °C of creating the LTP and above the melting temperature 271 °C of Bi. Moreover, to increase δ , the temperature-gradient driven annealing technique performed at 300 °C superimposed by $\text{grad}T = 2 \text{ }^\circ\text{C/cm}$ [9] was used instead of the conventional isothermal annealing technique. The optimal annealing time is 20 hours [9].

The arc-melted alloys were finely ground for obtaining the powder X-ray diffraction (PXRD) patterns. The LTP content δ was determined by using these PXRD patterns and the calibration curve method presented in [13]. The magnetic properties of MnBi alloys were estimated by measuring the loops of the isotropic and the in-epoxy-aligned powders.

The bulk magnets were prepared by using the MnBi powder of 5 μm average size. The powders were aligned in the magnetic field of 18 kOe and hot-compacted by the pressure P in the range of 600 ÷ 1800 psi at $T_a = 300 \text{ }^\circ\text{C}$ for $t_a = 10 \text{ min}$.

The anisotropy of magnets was checked by the texture of peaks appeared on the PXRD patterns taken on the magnet surface with the normal vector parallel (parallel surface) and perpendicular (perpendicular surface) to the direction of the aligning magnetic field. The anisotropy of magnets can be characterized by the ratio M_r/M_s estimated from the first quadrant loop section and the ratio iH_c/H_c representing the squareness γ estimated from the second quadrant loop section. The energy product $(BH)_{\max}$ has been also estimated from the second quadrant B-H loop section. The effects of the magnet processing on the $(BH)_{\max}$ will be analyzed in details.

3. RESULTS AND DISCUSSION

3.1. Estimation of LTP content δ

The phase composition of the $Mn_{50}Bi_{50}$ alloy prepared by the above mentioned technique is represented on its PXR pattern shown in Fig. 1.

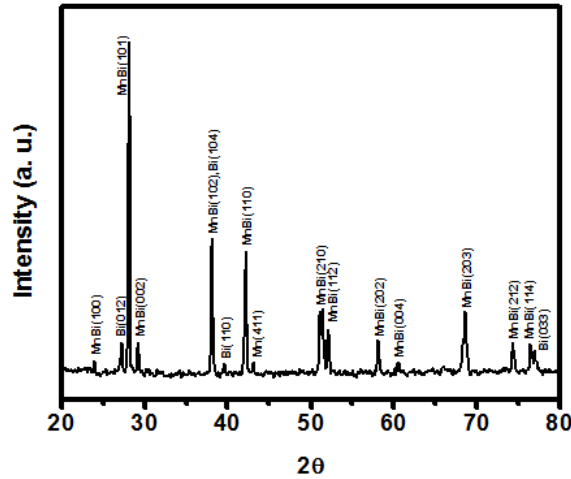


Figure 1. PXR pattern of the sample $Mn_{50}Bi_{50}$ alloyed by arc-melting and annealed at 300 °C superimposed by $gradT = 2$ °C/cm. The sample was finely ground to avoid any effect of the crystalline texture.

The peaks revealed that the sample consists of three phases of the LTP MnBi, Bi, and Mn. Since the sample was finely grounded, the peaks intensities correctly manifest the weighing ratio of these three phases. Among three strong peaks of LTP $MnBi_{(101)}$, $Bi_{(012)}$, $Mn_{(411)}$ the strongest peak is that of the LTP $MnBi_{(101)}$. The intensities of two peaks $Bi_{(012)}$ and $Mn_{(411)}$ were related by the ratio 1:3.8 which represents the ratio of the amounts of Bi and Mn excessive in the matrix of MnBi. The ratio α between the intensities of the peaks LTP $MnBi_{(101)}$ and $Bi_{(012)}$ equals 10.95, which corresponds to the content $\delta \sim 98$ wt% of LTP MnBi estimated from the calibration curve of the relation between δ and α as presented in [13]:

$$\delta(\text{wt}\%) = 44.63 + 51.3 \log \alpha.$$

3.2. Preparation of highly anisotropic magnets

A magnet is prepared from a hard magnetic material. Normally, the quality of magnets is of about 70 – 80 % of that of the material. The technology of preparing magnets is the process of optimal collecting magnetic grains to form a magnet product of wanted shape with high texture, high mass density and good balance between coercivity and remanence.

The arc-melted and annealed MnBi alloys were low-energy ball-milled by using the balls of 3 mm diameter, the weighing ratio of balls to powders is 10:1. The magnets were compacted in the non-magnetic mold. The powder grains loading to the mold were magnetized in a magnetic field of 18 kOe, and freely rotated under action of the field gradient and oriented parallel to the direction of this aligning field. The aligned grains were compacted by the pressure P ranged from 600 to 1800 psi and oriented perpendicularly to the aligning field direction. At this pressure P the green magnet compacts were sintered at 300 °C for 10 min. During the sintering, the Bi

excess was melted and functioned as a metal binder surrounding the MnBi grains to increase the magnet mass density and isolate the grains for controlling the magnet coercivity in the range 3 ÷ 7 kOe. Figure 2 presents the loops of the isotropic, in-epoxy aligned powder samples and of the prepared magnet, the pressure of 18000 psi was applied.

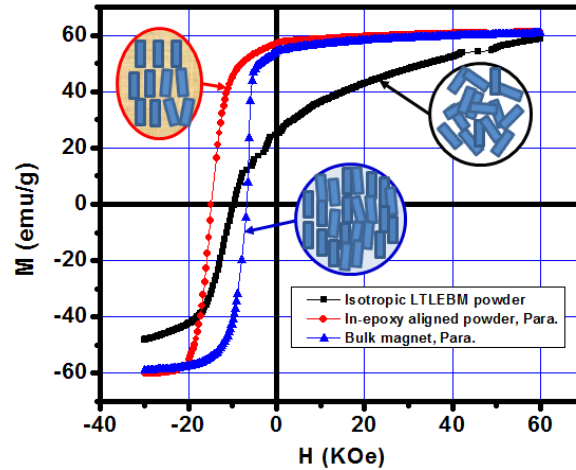


Figure 2. The magnetization loops of the isotropic powder sample (■), the in-epoxy aligned powder sample (●) and the bulk magnet sample (▲). In the two last cases the measuring field was parallel to the aligning direction. The insets model the grain microstructures of three samples.

In the isotropic sample, the grains were randomly oriented and this configuration was kept by the epoxy cover. The ratio M_r/M_s had the value of 0.44, which was close to the typical value of 0.5 of the Stoner-Wolfarth model for non-interactive single domain grains [14] with the easy axes randomly oriented in the 3D space of the space angle $\sigma = 180^\circ$.

In the in-diluted-epoxy aligned sample, each grain was covered by the thin epoxy layer, magnetized and freely rotated under action of a 18 kOe magnetic field while the epoxy resin was still liquid. This anisotropic configuration was kept until the epoxy has been cured and resulted in increasing the ratio M_r/M_s up to 0.92, which corresponds to the configuration of easy axes distributed in the space angle $\sigma \sim 20^\circ$ around the direction of the aligning field. Moreover, the relative distance between these magnetized grains was self-fixed by the balance of their repulsive forces, which corresponds to the energy minimum of a system of the same polarized grains. This configuration corresponds to the remanence $M_r = 58$ emu/g and the intrinsic coercivity $iH_c = 15$ kOe.

In the magnets described above, despite the limited space inside the mold, the grains can be freely rotated while they are loaded into the mold under action of a 18 kOe magnetic field, thus the texture of easy axes of loaded grains can be the same as of grains aligned in the epoxy. The final texture of grains can be disturbed by the compaction pressure P so the remanence M_r is decreased by a small amount in comparison with that of the in-epoxy aligned sample.

The 1800 psi in-mold compaction has small influence on the remanence M_r but significantly affects the coercivity iH_c by decreasing the value from 15 down to 7 kOe. This decline is caused by the disturbance of the balance of distances between the magnetized grains. Narrowing the inter-grain distance causes the increase of mass density (in comparison with that of the in-epoxy aligned sample). Hence, the system energy is increased and consequently the coercivity is reduced.

While the direct proportion between the pressure P and the magnet mass density ρ is repeatable, the reduction of iH_c caused by increasing P is only a trend because its stray energy contribution term depends strongly on the grain shape which is hardly controlled.

To estimate the P versus ρ dependence, the 10 gram arc-melted and annealed MnBi alloy sample was ball-milled and used for preparing magnets. For every batch, 1.5 grams of powders was loaded into the mold with the cross section area 8×10 mm. All the magnets were prepared by the same conditions except the value of the pressure P . The $\rho(P)$ is shown in Fig. 3.

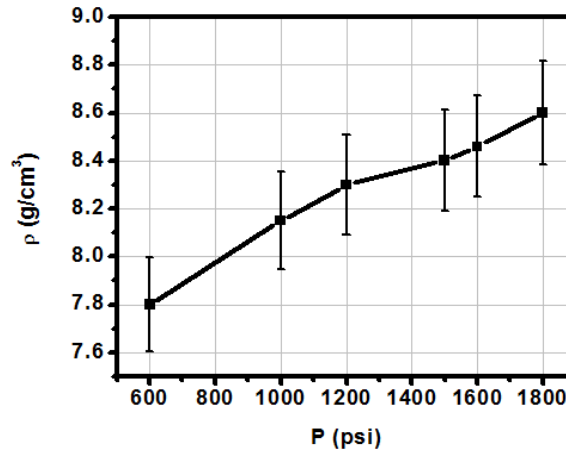


Figure 3. The dependence of the magnet mass density ρ on the compaction pressure P .

Within the standard deviation of the error, the function $\rho(P)$ can be considered as linear, the mass density ρ increased from 7.8 to 8.6 g/cm³ by increasing P from 600 to 1800 psi. The influence of the annealing temperature T_a on the magnet mass density is also observed. This effect is abrupt when T_a is over the melting temperature $T_m = 271$ °C of Bi. Three magnets were prepared by using the same conditions except the value of T_a , the density ρ equals 7 and 7.5 g/cm³ for $T_a = 220$ and 260 °C, respectively and sharply increases to 8.4 g/cm³ for $T_a = 300$ °C.

3.3. High-performance MnBi bulk magnets

MnBi bulk magnets were sintered in a Bi-excess medium. At 300 °C, Bi-excess is in the liquid state, and under action of the pressure P , Bi easily fills in voids and even moves out to the outer surface creating the magnet surface protection layer.

Figure 4 presents the magnetization loop of the high-performance magnet prepared by the route with following parameters: i) MnBi alloy was arc-melted and annealed to have LTP content $\delta = 97$ wt%; ii) this alloy was low-energy ball-milled into powders of average grain size of ~ 5 μm ; iii) the powder was aligned in a magnetic field of 18 kOe, hot-compacted by $P = 1500$ psi at $T_a = 300$ °C for $t_a = 10$ min.

The prepared magnet has the mass density $\rho = 8.4$ g/cm³, the ratio $M_r/M_s = 0.92$, the ratio $bH_c/iH_c = 0.89$ and $bH_c = 2.97$ kOe. The load line intersects the (BH) curve at $B_1 = 3.91$ kG and $H_1 = 2.16$ kOe. The energy product $(BH)_{\text{max}} = 8.4$ MGOe.

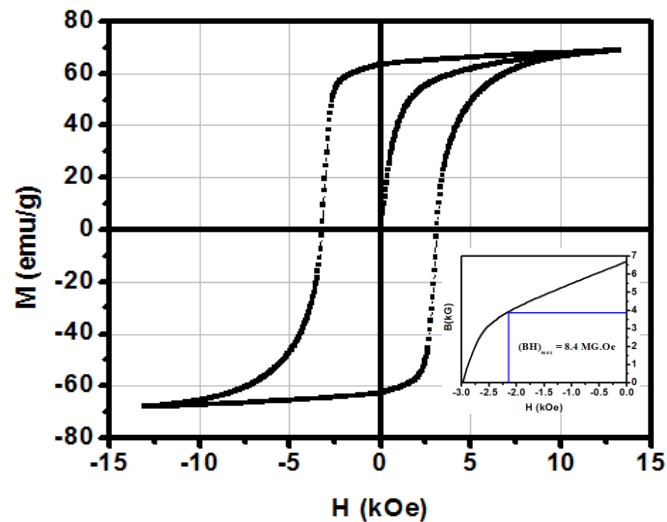


Figure 4. The magnetization loop of the high-performance MnBi magnet. The inset shows the curve $B(H)$ in the second quadrant.

The anisotropy of this magnet was clearly observed by comparing two XRD patterns taken on the magnet parallel and perpendicular surfaces. These XRD patterns are shown in Fig. 5.

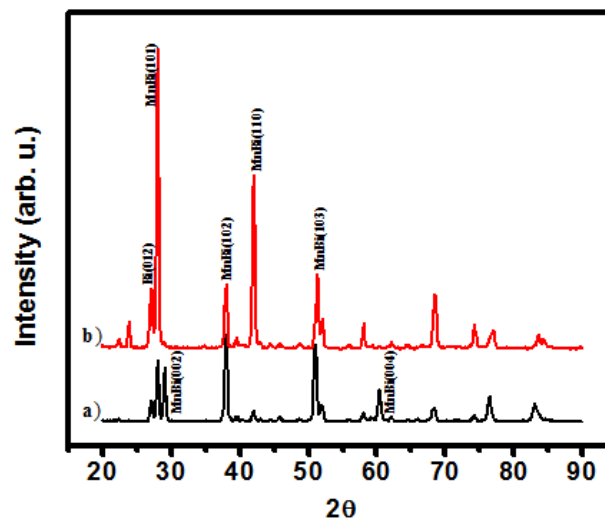


Figure 5. XRD patterns of the MnBi magnet with the loop presented in Fig. 4. The patterns were taken for the surfaces parallel (a) and perpendicular (b) to the direction of the aligning field H_a .

From Fig. 5, one can clearly see that the peaks belong to the LTPHase, except the peak (012) of Bi. The easy axes of grains are aligned along the direction of the aligning field H_a , thus the peaks (002) and (004) of LTPHase of MnBi were appeared clearly in the diagram (a) but unobservable in the diagram (b). Conversely, two peaks (101) and (110) of LTPHase of MnBi were appeared strongly in the diagram (b) since they correspond to the crystal planes perpendicular (the peak (110)) and nearly perpendicular (the peak (101)) to the easy axes (001).

4. CONCLUSION

The paper has presented a technology for preparation of high-performance MnBi bulk magnets. To prepare magnets, the starting material of the composition $\text{Mn}_{50}\text{Bi}_{50}$ was alloyed by the arc-melt, annealed at the temperature of 300 °C superimposed by the temperature gradient $\text{grad}T = 2 \text{ }^\circ\text{C}/\text{cm}$ for 20 hours. The alloy had high content of the ferromagnetic phase $\sim 98 \text{ wt}\%$ and was low-energy ball-milled to the powder of the average grain size $\sim 5 \text{ }\mu\text{m}$. The powder was aligned in a magnetic field of 18 kOe, hot-compacted at 300 °C for 10 min under pressure of 1500 psi. The prepared magnet had the high mass density $\rho = 8.4 \text{ g}/\text{cm}^3$, high anisotropy $M_r/M_s = 0.92$, large squareness $H_c/H_c = 0.89$ and high energy product $(\text{BH})_{\text{max}} = 8.4 \text{ MGOe}$. These results were obtained thanks to the technique of loading and rotating powder grains into the mold and the optimal compaction for maintaining the high anisotropy and balancing the remanence and coercivity of magnets. The cold ball-mil technique should be investigated to enhance further the coercivity without decreasing the remanence M_r and improve the energy product $(\text{BH})_{\text{max}}$ closely to 10 MGOe.

Acknowledgement: This research is funded by the Vietnam National Foundation for Science and Technology Development (NAFOSTED) under grant number 103.02-2014.28.

REFERENCES

1. Coey J. M. D. - Permanent magnets: Plugging the gap. *Scripta Materialia* **67** (2012) 524-529.
2. Chinnasamy C., Jasinski M. M., Ulmer A., Li W., Hadjipanayis G., and Liu J. - Mn-Bi Magnetic Powders With High Coercivity and Magnetization at Room Temperature. *IEEE Trans. Magn.* **48** (2012) 3641-3643.
3. Yang Y. B., Chen X. G., Wu R., Wei J. Z., Ma X. B., Han J. Z., Du H. L., Liu S. Q., Wang C. S., Yang Y. C., Zhang Y., and Yang J. B. - Preparation and magnetic properties of MnBi. *J. Appl. Phys.* **111** (2012) 07E312 (3 pp.).
4. Li Y. Q., Yue M., Zuo J. H., Zhang D. T., Liu W. Q., Zhang J. X., Guo Z. H., and Li W. - Investigation of Magnetic Properties of MnBi/Fe Nanocomposite Permanent Magnets by Micro-Magnetic Simulation *IEEE Trans. Magn.* **49** (2013) 3391-3393.
5. Olivetti E. S., Curcio C., Martino L., Küpferling M., Basso V. - Effect of Ti substitution on a and b phase formation and properties in $\text{Mn}_{50-x}\text{Ti}_x\text{Bi}_{50}$ alloys *J. Alloy Compd.* **643** (2015) S270-S274.
6. Adams E, Hubbard W. M., and Syeles A. M. – A New Permanent Magnet from Powdered Manganese Bismuthide. *J. Appl. Phys.* **23** (1952) 1207-1211.
7. Koa K. Y., Choi S. J., Yoon S. K., and Kwon Y. S. - MnBi magnets fabricated through spark plasma-sintering process. *J. Mag. Mag. Mat.* **310** (2007) e887–e889.
8. Rama Rao N. V., Gabay A. M. and Hadjipanayis G. C. - Anisotropic fully dense MnBi permanent magnet with high energy product and high coercivity at elevated temperatures. *J. Phys. D: Appl. Phys.* **46** (2013) 062001 (4pp).
9. Vuong N. V., Poudyal N., Liu X., Liu J. P., Kewei S., Kramer M. J., Cui J. - High-Performance MnBi Alloy Prepared Using Profiled Heat Treatment. *IEEE Trans. Magn.* **50** (2014) 2105506 (7 pp.).

10. Moon K. W., Jeon K. W., Kang M., Kang M. K., Byun Y., Kim J. B., Kim H., and Kim J. - Synthesis and Magnetic Properties of MnBi(LTP) Magnets With High-Energy Product IEEE Trans. Magn. **50** (2014) 2103804 (4 pp.)
11. Nguyen V. V., Poudyal N., Liu X., Liu J. P., Sun K., Kramer M. J., Cui J. - Novel processing of high-performance MnBi magnets. Mater. Res. Expr. **1** (2014) 036108 (10 pp.)
12. Massalski T. B. (Eds.) - Binary Alloy Phase Diagrams, ASM International, Materials Park, Ohio, 1990
13. Nguyen Xuan Truong and Nguyen Van Vuong, Preparation and magnetic properties of MnBi alloy and its hybridization with, Journal of Magnetism **20**(4) (2015) 1-6.
14. Coey J.M.D., Rare-Earth Iron Permanent-Magnets, "Chapter 3", Clarendon Press Oxford (1996).

TÓM TẮT

NAM CHÂM KHỐI MnBi CÓ TÍNH DỊ HƯỚNG CAO

Nguyễn Văn Vượng*, Nguyễn Xuân Trường

Viện Khoa học Vật liệu, Viện Hàn lâm KHCNVN, 18 Hoàng Quốc Việt, Cầu Giấy, Hà Nội

*Email: vuongnv@ims.vast.ac.vn

Vật liệu từ không chứa đất hiếm hệ MnBi được hứa hẹn dùng trong các ứng dụng của nam châm vĩnh cửu hoạt động tại vùng nhiệt độ cao 150 – 200 °C do chúng có năng lượng dị hướng tinh thể lớn và đặc biệt là hệ số nhiệt dương của trường kháng từ ($d_iH_c/dT > 0$). Do giá trị khiên tổn của từ độ bão hòa $M_s \sim 74$ emu/g, tính dị hướng của nam châm khối MnBi cần được nghiên cứu nâng cao để tạo ra từ độ dư M_r lớn. Với tỉ số M_r/M_s lớn và với một vi cấu trúc thích hợp, hệ số vuông góc γ của nam châm MnBi sẽ đạt giá trị cao khiến trường kháng từ H_c tiệm cận gần đến H_c và do đó tích năng lượng từ $(BH)_{max}$ được nâng cao. Bài báo trình bày một phương thức ép dị hướng nam châm MnBi trong từ trường 18 kOe có phương vuông góc với lực ép mà tại đó các hạt từ cứng MnBi được xoay hầu như tự do và định hướng dọc theo hướng của từ trường. Lực ép viên nam châm được lựa chọn thích hợp trên cơ sở tối thiểu hóa năng lượng của hệ các hạt từ cứng sau khi được nhiễm từ để tối ưu hóa hai tham số, tỉ trọng ρ và trường kháng từ H_c của nam châm. Nam châm MnBi chế tạo được có $\rho \sim 8,4$ g/cm³, $M_r/M_s \sim 0,92$, $\gamma \sim 0,89$ và $(BH)_{max}$ đạt giá trị $\sim 8,4$ MG.Oe.

Từ khóa: nam châm không chứa đất hiếm MnBi, tính dị hướng, ép dị hướng nam châm.